
Do the various types of Low Ionization Structures of PNe differ in terms of their physical parameters?

Denise R. Gonçalves

Observatório do Valongo - UFRJ
Ladeira Pedro Antonio, 43 - 200080-090 Rio de Janeiro, Brazil
denise@ov.ufrj.br

Summary. Years ago Gonçalves et al. (2001) compiled all the available optical data in the literature to build a comprehensive classification of the low-ionization structures (LIS) of PNe in terms of their morphology (narrow-band imaging) and kinematics (long-slit spectroscopy). This classification highlighted a number of questions that years later still remain open, such as, what is the role of magnetic fields and of the binary systems on the formation of collimated LIS, or, how do collimated low-velocity LIS survive throughout the PNe evolution? Other works also called our attention to the unexpected fact that highly supersonic LIS are mainly photoionized (e.g., in NGC 7662 and NGC 7009) and that no significant density contrasts were found between collimated LIS and their environment. In an attempt to provide an answer to these and other questions raised by previous works we have undertaken a systematical exploration of the physical properties of the LIS. We obtained optical long-slit spectra of a sample of PNe with LIS covering all the different LIS types and PNe morphologies. Here we show the results for 12 of the PNe in the sample. We have estimated the electronic temperature, T_e , and density, N_e , of the LIS and compare them with the T_e and N_e of their surrounding nebula. Here we discuss our newly found correlations between the different types of LIS, their physical parameters and the current scenarios that try to explain their existence.

Key words: Planetary Nebulae: individual (NGC 7009, NGC 6543, K 4-47, NGC 6891, NGC 6881, K 1-2, He 2-429, IC 4593, IC 2149, He 1-1, KJpN8, NGC 7662).

1 LIS: previous knowledge

We are involved in a long-term project for characterizing the small-scale low-ionization structures of PNe since they can tell us much about the formation and evolution of PNe. The main issues we can access by studying the LIS are:

1. the collimation processes of LIS as well as those processes responsible for the shape of the PN itself;
2. the effect of the ionization front (IF) on the fossil AGB features;

3. the mass-loss processes during the AGB and post-AGB phases; and
4. whether or not disks and magnetic fields are needed to explain the highly collimated outflows (jets) in PNe.

All of these are old issues (raised at the time of the first B. Balick's paper in this field; i.e. Balick et al. 1993), which need to be properly addressed. Partial responses to these questions were given for a few PNe, but until now there is no clear scenario for the formation and evolution of most LIS. On top of these issues is the doubt: does the presence of LIS affect the chemical enrichment given by low- to intermediate-mass stars?

So far, we have investigated different aspects of LIS in this project, such as, the optical morphology and kinematics of LIS (Corradi et al. 1999, 2000a, 2000b; Gonçalves et al. 2001; Gonçalves 2004), the physical and chemical properties of a few PNe that contain LIS (Gonçalves et al. 2003, 2004, 2006; Gonçalves 2004); and we just started to investigate the LIS in the near-IR.

As a resume of what we already know about these structures (knots, jets and jetlike¹ systems, either in pairs or isolated) we may affirm that: i) around 10% of the Galactic PNe are known to possess LIS; ii) they are indistinctly spread among all the PNe morphological classes; iii) 50% of these PNe have highly collimated, high-velocity jets, and/or high-velocity pairs of knots (FLIERs); iv) most of them are mainly photoionized (Gonçalves et al. 2001; Gonçalves 2004).

2 The Present Survey: LIS physical properties

This survey is based on long-slit optical spectroscopy, of medium resolution, taken at the 2.5m Isaac Newton Telescope. The spectral coverage, reciprocal dispersion and spatial resolution of the spectra are 3650Å to 7000Å, 3.11Å per pixel, and 0.70'' per pixel, respectively. Figures 1-3 show the 12 PNe whose results are discussed here. They are grouped in accordance with the three types of LIS observed in these PNe, which are, respectively, pairs of jets, jetlike structures and knots.

Diagnostic emission line ratios we adopt for this analysis –roughly representing the low- as well as high-ionization regions within a typical PN– are: $N_e[\text{S II}] \propto I(6717\text{Å})/I(6737\text{Å})$; $N_e[\text{Cl III}] \propto I(5517\text{Å})/I(5537\text{Å})$; $T_e[\text{O III}] \propto I(4959\text{Å}+5007\text{Å})/I(4363\text{Å})$; $T_e[\text{N II}] \propto I(6548\text{Å}+6583\text{Å})/I(5755\text{Å})$; and $T_e[\text{S II}] \propto I(6717\text{Å}+6737\text{Å})/I(4069\text{Å}+4076\text{Å})$.

Our results are shown in Tables 1-13. These tables give the N_e and T_e of all the structures we were able to measure along each slit. In some cases the physical parameters that correspond to the integrated emission along the slit (i.e., the entire nebula) are also given in the last column. Please refer to Figures 1-3 for the identification of the structures in the tables. In the tables, values of T_e quoted as 21,000 K indicate lower limits for actual temperatures.

Our main goal is to use this survey to address the following: do the various types of LIS differ in terms of their physical properties? From a close analysis of the figures given in Tables 1-13 we characterize the different small-scale structures in the following way:

¹ These are features that resemble highly supersonic jets, but that share the expansion of the nebular components in which they are embedded.

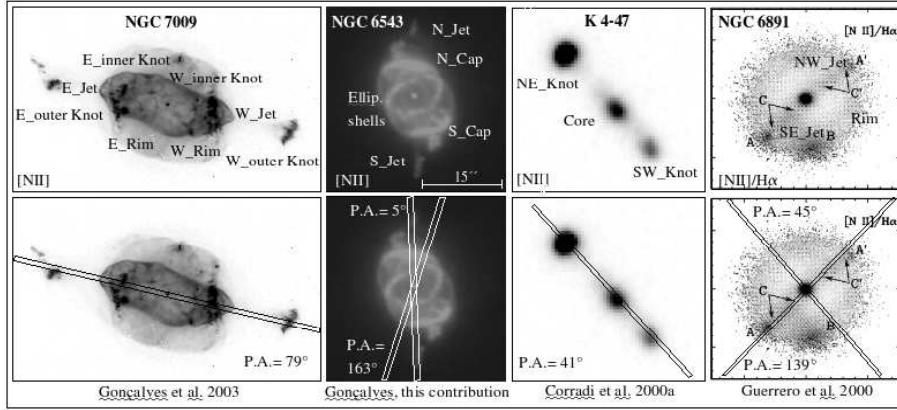


Fig. 1. PNe with highly supersonic jets: NGC 7009; NGC 6543; K 4-47 and NGC 6891. *Top:* In these panels the label of the different structures under analysis are given. Values for T_e and N_e are given in Tables 1-4. The $[\text{N II}]$ images of NGC 7009 and K 4-47 were adapted from Fig.1 of Gonçalves et al. (2003) and Fig.6 of Corradi et al. (2000a), respectively. The $[\text{N II}]/\text{H}\alpha$ image of NGC 6891 was adapted from Fig.1 of Guerrero et al. (2000). *Bottom:* In these panels we show, superposed to the images, a sketch of the long-slits used, as well as their respective position angles (P.A.). All images are oriented with North up and East to the left. See quoted references for the images scale.

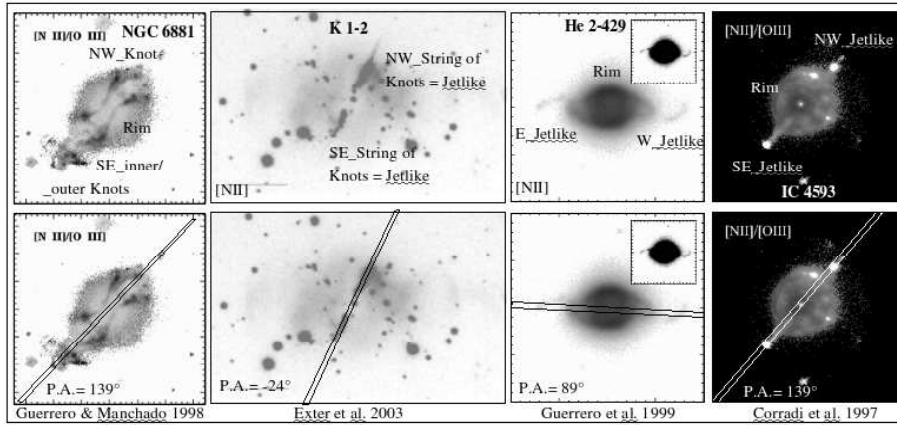


Fig. 2. PNe with jetlike pairs: NGC 6881; K 1-2; He 2-429 and NGC 4593. *Top:* as in Fig.1, but for Tables 5-8. The $[\text{N II}]/[\text{O III}]$ images of NGC 6881 and IC 4593 were adapted from Fig.1 of Guerrero & Manchado (1998) and Fig.1 of Corradi et al. (1997), respectively. The $[\text{N II}]$ images of K 1-2 and He 2-429 were adapted from Fig.2 of Exter et al. (2003) and Fig.1 of Guerrero et al. (1999). *Bottom:* as in Fig.1.

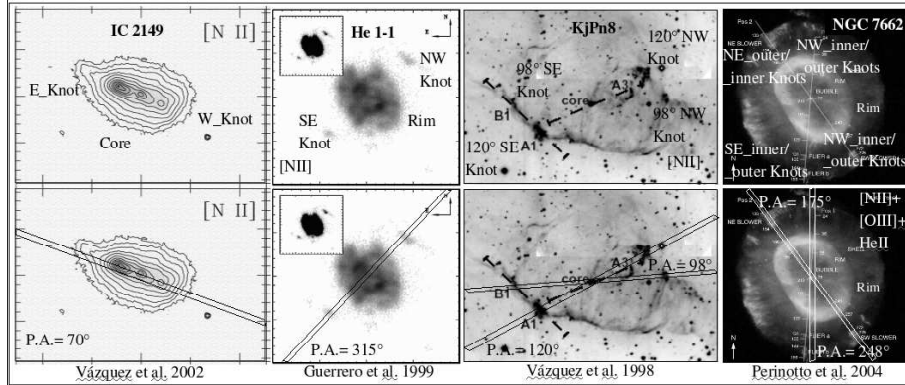


Fig. 3. PNe with pairs of knots: IC 2149; He 1-1; KJPn8 and NGC 7662. *Top:* as in Fig.1, but for Tables 9-13. The [N II] images of the PNe shown here were adapted from Fig.1. of Vázquez et al. (2002), Fig.1 of Guerrero et al. (1999), Fig.1 of Vázquez et al. (1998) and Fig.1 of Perinotto et al. (2004), corresponding to IC 2149, He 1-1, KJPn8 and NGC 7662, respectively. *Bottom:* as in Fig.1.

Jets: their densities are lower than the densities of their tips (the bright knots like those in NGC 7009) by a factor of ~ 2 . Note that the shock excited knots in K 4-47 are an exception to this rule. T_e are usually similar for all the features of the PN. Can the lower N_e of the jets as compared to the tips be accounted for by the theoretical models? A preliminary answer is: possibly yes, since jets can be fully ionized, and therefore the N_e we derive represent their actual densities, whereas their tips can be partially neutral, so that the N_e diagnostics used do not represent their real densities.

Jetlike: in addition to the unexpected fact that these are well collimated structures of low-velocity, the jetlike LIS also have densities that are lower than the surrounding medium by a factor of ~ 2 , and in some cases slightly high T_e . Note, however, that in general the temperatures of the jetlike systems are hard to measure (see Tables 6 and 7). Anyway, the T_e of these structures are not as high as those of the shock excited knots. Is this a relevant constraint for modeling?

Knots: FLIERS (fast moving knots) and SLOWERS (slowly moving knots), as well as jets and jetlike LIS, are not significantly different from each other in terms of T_e and N_e . This is hard to understand, because we do not know how to keep low-velocity features collimated. The situation is further complicated by the fact that no significant density contrasts were found in between FLIERS, SLOWERS and their environments.

References

1. Balick B., Rugers M., Terzian Y., & Chengalur J.N., 1993, ApJ, 411, 778
2. Corradi R.L.M., Guerrero M., Manchado A., & Mampaso A., 1997, NewA, 2, 461

3. Corradi R.L.M., Perinotto M., Villaver E., Mampaso A., & Gonçalves D.R., 1999, ApJ, 523, 721
4. Corradi R.L.M., Gonçalves D.R., Villaver E., Mampaso A., & Perinotto M., 2000a, ApJ, 542, 861
5. Corradi R.L.M., Gonçalves D.R., Villaver E., Mampaso A., Perinotto M., Schwarz H.E., & Zanin C., 2000b, ApJ, 535, 823
6. Exter K.M., Pollacco D.L., Bell S.A., 2003, MNRAS, 341, 1349
7. Gonçalves D.R., Corradi R.L.M., & Mampaso A., 2001, ApJ, 547, 302
8. Gonçalves D.R., Corradi R.L.M., Mampaso A., & Perinotto M., 2003, ApJ, 597, 975
9. Gonçalves D.R., 2004, ASP Conference Series, vol. 313, p.216
10. Gonçalves D.R., Mampaso A., Corradi R.L.M., Perinotto M., Riera A., & López-Martín L., 2004, MNRAS, 355, 37
11. Gonçalves D.R., Ercolano B., Carnero A., Mampaso A., & Corradi R.L.M., 2006, MNRAS, 365, 1039
12. Guerrero M.A., & Manchado A., 1998, ApJ, 508, 262
13. Guerrero M.A., Vázquez R., & López J.A., 1999, AJ, 117, 967
14. Guerrero M.A., Miranda L.F. Manchado A., & Vázquez R., 2000, MNRAS, 313, 1
15. Perinotto M., Patriarchi P., Balick B., & Corradi R.L.M., 2004, A&A, 422, 963
16. Vázquez R., Kingsburgh R.L., & López J.A., 1998, MNRAS, 296, 564
17. Vázquez R., Miranda L.F., Torrelles J.M., Olguín L., Benítez G., Rodríguez L.F., & López J.A., 2002, ApJ, 576, 860

Table 1. NGC 7009: N_e and T_e . (Structures are defined in Fig.1; P.A.=79°)

Parameter	Rim		Knots				Jets	
	Eastern	Western	E_outer	E_inner	W_inner	W_outer	Eastern	Western
$N_e[\text{S II}](\text{cm}^{-3})$	5,500	5,900	2,000	4,500	5,000	1,300	1,300	1,100
$N_e[\text{Cl III}](\text{cm}^{-3})$	5,200	5,900	-	4,700	6,000	1,900	-	1,300
$T_e[\text{O III}](\text{K})$	10,000	10,200	9,600	9,300	10,100	10,400	10,400	11,600
$T_e[\text{N II}](\text{K})$	10,400	12,800	11,000	9,400	10,400	11,700	-	-
$T_e[\text{S II}](\text{K})$	-	-	7,100	8,300	-	9,400	-	-

Table 2. NGC 6543: N_e and T_e . (As in Table 1, with P.A.= 5° and 163°)

Parameter	Jets		Caps		Ellip. Shells	
	Northern	Southern	Northern	Southern	Northern	Southern
$N_e[\text{S II}](\text{cm}^{-3})$	2,000	1,150	9,150	5,550	7,350	7,050
$N_e[\text{Cl III}](\text{cm}^{-3})$	6,900	2,550	9,350	4,750	5,500	6,100
$T_e[\text{O III}](\text{K})$	9,850	9,250	7,950	7,600	8,100	7,750
$T_e[\text{N II}](\text{K})$	7,600	7,000	8,450	9,000	9,250	9,350
$T_e[\text{S II}](\text{K})$	9,250	7,150	10,700	7,550	-	-

Table 3. K 4-47: N_e and T_e . (As in Table 1, with P.A.= 41°)

Parameter	Core	Knots		NEB
		NE	SW	entire PN
$N_e[\text{S II}](\text{cm}^{-3})$	1,900	4,550	2,450	2,800
$N_e[\text{Cl III}](\text{cm}^{-3})$	-	-	-	-
$T_e[\text{O III}](\text{K})$	19,300	21,000	16,100	19,300
$T_e[\text{N II}](\text{K})$	21,000	18,900	16,950	20,600
$T_e[\text{S II}](\text{K})$	-	-	-	-

Table 4. NGC 6891: N_e and T_e . (As for in Table 1, with P.A.= 45° and 135°)

Parameter	Rim		Jets		NEB
	NE	SW	SE	NW	entire PN
$N_e[\text{S II}](\text{cm}^{-3})$	1,950	1,000	1,400	1,100	1,250
$N_e[\text{Cl III}](\text{cm}^{-3})$	-	900	2,100	2,700	-
$T_e[\text{O III}](\text{K})$	10,200	9,950	8,650	9,500	9,550
$T_e[\text{N II}](\text{K})$	9,450	9,450	9,050	10,300	9,612
$T_e[\text{S II}](\text{K})$	-	-	-	-	-

Table 5. NGC 6881: N_e and T_e . (Structures are defined in Fig.2; P.A.= 139°)

Parameter	Rim	Knots		NEB	
		SE_inner	SE_outer	NW	entire PN
$N_e[\text{S II}](\text{cm}^{-3})$	9,700	750	1,900	650	7,700
$N_e[\text{Cl III}](\text{cm}^{-3})$	-	-	-	-	-
$T_e[\text{O III}](\text{K})$	12,750	-	-	-	13,450
$T_e[\text{N II}](\text{K})$	14,350	-	-	21,000	15,050
$T_e[\text{S II}](\text{K})$	-	-	-	-	-

Table 6. K 1-2: N_e and T_e . (As in Table 5, with P.A.= -24°)

Parameter	NW_String of Knots			SE_String of Knots			NEB entire PN	
	NW _a	NW _b	NW _c	NW _d	SE _e	SE _f		SE _g
$N_e[\text{S II}](\text{cm}^{-3})$	1,000	600	1,000	-	-	450	1,450	500
$N_e[\text{Cl III}](\text{cm}^{-3})$	-	-	-	-	-	-	-	-
$T_e[\text{O III}](\text{K})$	-	15,700	14,000	-	-	-	-	14,9000
$T_e[\text{N II}](\text{K})$	-	-	-	-	-	-	-	11,000
$T_e[\text{S II}](\text{K})$	-	-	-	-	-	-	-	-

Table 7. He 2-429: N_e and T_e . (As in Table 5, with P.A.= 89°)

Parameter	Rim	Jetlike		NEB entire PN
		Eastern	Western	
$N_e[\text{S II}](\text{cm}^{-3})$	7,900	3,200	3,550	7,550
$N_e[\text{Cl III}](\text{cm}^{-3})$	-	-	-	-
$T_e[\text{O III}](\text{K})$	8,700	-	-	8,700
$T_e[\text{N II}](\text{K})$	-	-	-	4,300
$T_e[\text{S II}](\text{K})$	-	-	-	-

Table 8. IC 4593: N_e and T_e . (As in Table 5, with P.A.= 139°)

Parameter	Jetlike		Rim		NEB entire PN	
	SE	NW	SE	Central		
$N_e[\text{S II}](\text{cm}^{-3})$	900	1,700	3,150	2,150	1,650	2,350
$N_e[\text{Cl III}](\text{cm}^{-3})$	-	-	3,050	1,500	-	1,800
$T_e[\text{O III}](\text{K})$	12,600	10,350	9,700	7,850	7,400	8,200
$T_e[\text{N II}](\text{K})$	20,450	-	11,500	9,350	-	9,950
$T_e[\text{S II}](\text{K})$	-	-	-	-	-	-

Table 9. IC 2149: N_e and T_e . (Structures are defined in Fig.3; P.A.= 70°)

Parameter	Core	Knots		NEB entire PN
		Eastern	Western	
$N_e[\text{S II}](\text{cm}^{-3})$	6,000	5,000	2,100	4,200
$N_e[\text{Cl III}](\text{cm}^{-3})$	-	8,000	2,550	1,800
$T_e[\text{O III}](\text{K})$	11,350	10,300	9,800	11,200
$T_e[\text{N II}](\text{K})$	10,400	10,900	12,450	10,200
$T_e[\text{S II}](\text{K})$	-	-	7,600	9,550

Table 10. He 1-1: N_e and T_e . (As in Table 9, with P.A.=315°)

Parameter	Rim	Knots		NEB
		SE	NW	entire PN
$N_e[\text{S II}](\text{cm}^{-3})$	1,600	650	1,300	1,550
$N_e[\text{Cl III}](\text{cm}^{-3})$	-	-	-	-
$T_e[\text{O III}](\text{K})$	12,050	21,000	-	12,800
$T_e[\text{N II}](\text{K})$	10,750	10,400	-	10,600
$T_e[\text{S II}](\text{K})$	16,400	-	-	-

Table 11. KJpN8: N_e and T_e . (As in Table 9, with P.A.=98° and 120°)

Parameter	PA=98°		PA=120°	
	SE_Knot	NW_Knot	SE_Knot	NW_Knot
$N_e[\text{S II}](\text{cm}^{-3})$	600	600	500	500
$N_e[\text{Cl III}](\text{cm}^{-3})$	-	-	300	-
$T_e[\text{O III}](\text{K})$	21,000	20,600	21,000	21,000
$T_e[\text{N II}](\text{K})$	-	8,700	10,050	8,300
$T_e[\text{S II}](\text{K})$	-	-	14,200	11,500

Table 12. NGC 7662: N_e and T_e . (As in Table 9, with P.A.=175° – FLIERs)

Parameter	Knots		Rim	Knots		
	SE_outer	SE_inner		NW_inner	NW_outer	entire PN
$N_e[\text{S II}](\text{cm}^{-3})$	1,300	3,500	2,550	4,050	1,750	3,250
$N_e[\text{Cl III}](\text{cm}^{-3})$	800	3,200	-	3,600	850	2,150
$T_e[\text{O III}](\text{K})$	12,400	13,200	14,850	14,550	13,650	13,700
$T_e[\text{N II}](\text{K})$	12,000	8,450	-	13,650	14,650	-
$T_e[\text{S II}](\text{K})$	-	-	-	-	-	-

Table 13. NGC 7662: N_e and T_e . (As in Table 9, with P.A.=248° – SLOWERs)

Parameter	Knots		Rim	Knots		
	NE_outer	NE_inner		SW_inner	SW_outer	entire PN
$N_e[\text{S II}](\text{cm}^{-3})$	2,350	3,600	2,850	5,000	2,600	2,900
$N_e[\text{Cl III}](\text{cm}^{-3})$	2,400	3,950	1,700	3,500	1,150	3,100
$T_e[\text{O III}](\text{K})$	12,200	13,050	13,500	13,200	12,350	12,950
$T_e[\text{N II}](\text{K})$	-	11,800	11,550	10,600	11,550	10,950
$T_e[\text{S II}](\text{K})$	-	-	-	-	-	-